Artemisia annua mutant impaired in artemisinin synthesis demonstrates importance of nonenzymatic conversion in terpenoid metabolism

Tomasz Czechowski[a], Tony R. Larson[a], Theresa M. Catania[a], David Harvey[a], Geoffrey D. Brown[b], and Ian A. Graham[a,1]

[a]Centre for Novel Agricultural Products, Department of Biology, University of York, Heslington, York YO10 5DD, United Kingdom; and [b]Department of Chemistry, University of Reading, Reading RG6 6AD, United Kingdom

Edited by Chris R. Somerville, University of California, Berkeley, CA, and approved November 7, 2016 (received for review July 22, 2016)

Artemisinin, a sesquiterpene lactone produced by *Artemisia annua* glandular secretory trichomes, is the active ingredient in the most effective treatment for malaria currently available. We identified a mutation that disrupts the amorpha-4,11-diene C-12 oxidase (CYP71AV1) enzyme, responsible for a series of oxidation reactions in the artemisinin biosynthetic pathway. Detailed metabolic studies of *cyp71av1-1* revealed that the consequence of blocking the artemisinin biosynthetic pathway is the redirection of sesquiterpene metabolism to a sesquiterpene epoxide, which we designate arteannuin X. This sesquiterpene approaches half the concentration observed for artemisinin in wild-type plants, demonstrating high-flux plasticity in *A. annua* glandular trichomes and their potential as factories for the production of novel alternate sesquiterpenes at commercially viable levels. Detailed metabolite profiling of leaf maturation time-series and precursor-feeding experiments revealed that nonenzymatic conversion steps are central to both artemisinin and arteannuin X biosynthesis. In particular, feeding studies using ^{13}C-labeled dihydroartemisinic acid (DHAA) provided strong evidence that the final steps in the synthesis of artemisinin are nonenzymatic in vivo. Our findings also suggest that the specialized subapical cavity of glandular secretory trichomes functions as a location for both the chemical conversion and the storage of phytotoxic compounds, including artemisinin. We conclude that metabolic engineering to produce high yields of novel secondary compounds such as sesquiterpenes is feasible in complex glandular trichomes. Such systems offer advantages over single-cell microbial hosts for production of toxic natural products.

artemisinin | p450 oxidase | terpenoid | sesquiterpene | *Artemisia annua*

The sesquiterpene lactone artemisinin is the active ingredient in artemisinin-combination therapies—the most effective treatment for malaria currently available. The production of artemisinin occurs in specialized 10-cell biseriate glandular trichomes present on the leaves, stems, and inflorescences of *Artemisia annua* (1–3). Artemisinin is phytotoxic (4) and is believed to accumulate in the subapical extracellular cavity of glandular trichomes (2). This ability of trichomes to transfer compounds into extracellular cavities (5, 6) overcomes the problem of cellular toxicity. Conveniently, natural products located in these cavities are readily extractable as exemplified by artemisinin. This natural product is extracted on a commercial scale by submerging intact dried *A. annua* leaf material in organic solvent with the active ingredient being directly crystallized from the condensed organic fraction (7). There has been much interest in determining the steps involved in the biosynthesis of artemisinin in recent years, largely driven by efforts to produce this compound through a completely biosynthetic microbial-based fermentation route (8, 9). Presently microbial production is at best semisynthetic, terminating at artemisinic acid (AA), which must then be extracted from culture and chemically converted to artemisinin by using photooxidation (8, 10). The lack of a low-cost, scalable conversion process is considered to be a major factor in the failure so far of the semisynthetic route to sustainably impact the market, making it uncompetitive with plant-based production (11).

Although the enzymatic steps involved in production of the nonphytotoxic precursors amorpha-4,11-diene (A-4,11-D) and dihydroartemisinic acid (DHAA) have been elucidated (12–15) and the associated genes have been shown to be highly expressed in both the apical and subapical cells of the glandular secretory trichomes (3, 16), the final steps in the conversion of DHAA to artemisinin are considered to be nonenzymatic and may be extracellular (17, 18). Therefore, microbial-based "complete" synthetic biology routes to artemisinin may never be achievable. Meanwhile, modern molecular breeding has succeeded in improving *A. annua* (19), creating hybrids reaching artemisinin yields of 1.4% dry leaf biomass in commercial field trials (20) (www.artemisiaf1seed.org/).

The glandular secretory trichomes of *A. annua* produce almost 600 secondary or specialized metabolites, many of which are terpenoids (21). These include a significant number of terpene allylic hydroperoxides and endoperoxides (21). This latter class, of which artemisinin is a member, are typically bioactive and therefore potential targets for development as pharmaceuticals (22). Consistent with their phytochemical complexity, it is known that glandular secretory trichomes express multiple members of gene families, encoding enzymes of specialized metabolism, including terpene synthases and cytochrome P450 oxidases (16, 19, 23). Many of these enzymes are considered to be promiscuous (24). We reasoned that this plasticity could be exploited by developing biochemical knockouts, redirecting flux to new high-value sesquiterpenes in a proven plant production system.

Recent attempts to knock down the A-4,11-D synthase by using RNAi in self-pollinating *A. annua* resulted in only a modest (30–50%) reduction in artemisinin levels (25). We have chosen to target amorpha-4,11-diene C-12 oxidase (CYP71AV1), which catalyzes the three-step conversion of A-4,11-D to AA (13, 26, 27).

Significance

The antimalarial artemisinin is a sesquiterpene lactone produced by glandular secretory trichomes on the leaves of *Artemisia annua*. Using a mutant impaired in artemisinin synthesis, we demonstrate the importance of nonenzymatic conversions in terpenoid metabolism and highlight the ability of *A. annua* glandular secretory trichomes to redirect flux into a sesquiterpene epoxide. The research presented offers insight into the mechanism of the final steps of artemisinin synthesis in *A. annua*, with significant implications for future production of secondary compounds in native versus heterologous host systems.

Author contributions: T.C. and I.A.G. designed research; T.C., T.M.C., D.H., and G.D.B. performed research; T.C., T.R.L., T.M.C., G.D.B., and I.A.G. analyzed data; and T.C. and I.A.G. wrote the paper.

The authors declare no conflict of interest.

This article is a PNAS Direct Submission.

Freely available online through the PNAS open access option.

[1]To whom correspondence should be addressed. Email: ian.graham@york.ac.uk.

This article contains supporting information online at www.pnas.org/lookup/suppl/doi:10.1073/pnas.1611567113/-/DCSupplemental.

When we knocked out this enzyme, as expected, artemisinin was not produced; however, rather than A-4,11-D accumulating, it was instead readily converted to a sesquiterpene epoxide, arteannuin X. Detailed metabolite analysis revealed that production of this compound paralleled the production of artemisinin during leaf maturation, with early steps occurring in young leaves and later steps in older leaves. Our findings confirm the function of the CYP71AV1 enzyme in planta and also demonstrate the flexibility of glandular secretory trichome biochemistry, such that it is capable of redirecting the flux of A-4,11-D into a sesquiterpene epoxide at levels similar to artemisinin.

Results and Discussion

Disruption of *CYP71AV1* Results in the Accumulation of a Sesquiterpene Epoxide at the Expense of Artemisinin. We used the TILLING method (28) to screen for mutations in the single-copy (Fig. S1) *CYP71AV1* gene in an F2 population of *A. annua* that had been derived from an ethyl methane sulfonate (EMS)-mutagenized population of the Artemis F1 hybrid, as described (19). This process resulted in an allelic series of 10 mutants, of which just 1 was nonsense because of a G-to-A transition in the second exon of *CYP71AV1* (Fig. S2*A*). This mutation, which we designate *cyp71av1-1*, gives a predicted conversion of amino acid Trp-124 in the polypeptide to a stop codon, resulting in a major truncation of the enzyme and loss of most of the putative heme-binding sites, as well as Ser-473, which is crucial for catalyzing oxidation reactions (Fig. S2 *B* and *C*).

Previous work had shown that early stage intermediates in the artemisinin pathway accumulate in young *A. annua* leaves, and, as they mature, artemisinin accumulates (25, 29). To investigate the effects of the *cyp71av1-1* mutation on artemisinin biosynthesis, we analyzed three leaf developmental stages: juvenile (leaves 1–5 as counted down from the apical meristem), expanding (leaves 7–9), and mature (leaves 11–13). To generate material for this analysis, we backcrossed *cyp71av1-1 to Artemis* parents, selfed the progeny, and performed DNA marker-based selection of wild-type (WT), heterozygous, and homozygous *cyp71av1-1* individuals from the segregating backcrossed F2 population (Fig. S3). We did not detect any morphological differences between WT and *cyp71av1-1* material (Fig. S4). We also extended the analysis to include oven-dried leaf material stripped from entire plants to investigate metabolite conversions occurring after harvest.

Compared with WT and heterozygous material, the juvenile leaves of *cyp71av1-1* contain significantly elevated levels of the first committed metabolite in the artemisinin pathway, A-4,11-D (Fig. 1 *A*, *i* and Dataset S1), consistent with the reported in vitro activity of CYP71AV1 (13, 26, 27). Metabolite profiling further revealed a complete loss of all metabolites downstream of A-4,11-D including artemisinin, which typically accumulate in juvenile, expanding and mature WT leaves (Fig. 1 *A*, *ii–viii* and *C* and Datasets S2 and S3).

Other classes of secondary metabolites, including aromatic alcohols and ketones, coumarins, monoterpenes, and other sesquiterpenes remained largely unchanged in *cyp71av1-1* (Datasets S1 and S3). However, levels of some minor monoterpenes (eucalyptol, borneol, and sabinene) and sesquiterpenes (calarene, α-bisabolol, and cedrenol,) were reduced, and levels of two minor flavonoids (retusin and artemetin) were increased in *cyp71av1-1* (Datasets S1 and S3). These and other changes were largely restricted to the juvenile leaves (Datasets S1 and S3 and Fig. S5), which are relatively dense in glandular trichomes (29) and exhibit high expression levels of terpene synthases (30). Recent attempts to silence *AMORPHA-4,11-DIENE SYNTHASE* expression in self-pollinating varieties of *Artemisia annua* resulted in increased levels of two nonamorphadiene sesquiterpenes, caryophyllene and copaene, which may be due to an elevated pool of farnesyl diphosphate acting as substrate for other sesquiterpene synthases in the glandular trichomes (25).

Ultraperformance liquid chromatography tandem mass spectrometry (UPLC-MS) analysis revealed that *cyp71av1-1* leaves accumulate large amounts of an oxygenated C_{14} metabolite (Dataset S3, Peak_ID M221.1535T43). One-dimensional (1D) and 2D NMR (spectroscopic techniques were used to elucidate the structure of this amorphadiene sesquiterpene as (2*S*,3*R*,6*S*)-3-methyl-6-(2*R*-methyloxiran-2-yl)-2-(3-oxobutyl) cyclohexanone, which we refer to as arteannuin X (Fig. 1 *A*, *ix* and *B*). At 0.4% leaf dry weight in mature leaves the concentration of arteannuin X in *cyp71av1-1* is almost half that of artemisinin in WT leaves and the developmental profile for accumulation in expanding and mature leaves is similar for both compounds (Fig. 1 *A*, *ix* and Dataset S3). The fact that arteannuin X is present in trace amounts in WT and heterozygous *cyp71av1-1* material (Fig. 1 *A*, *ix* and Dataset S3) suggests that it normally occurs as a by-product of A-4,11-D oxidation. In vivo and in vitro formation of low abundance by-products derived from other intermediates of artemisinin synthesis have been reported (12, 17, 18).

NMR analysis of *cyp71av1-1* extracts identified a second major compound, A-4,11-D tertiary allylic hydroperoxide (A-4,11-DOOH; Fig. 1 *A*, *x* and *B*) that had not previously been reported in WT *A. annua*. The pattern of accumulation of A-4,11-DOOH (Fig. 1 *A*, *x*) preempted that of arteannuin X reaching a concentration of almost 0.15% leaf dry weight in juvenile and expanding leaves of *cyp71av1-1* before decreasing in mature leaves (Fig. 1 *A*, *x*). Although A4,11-DOOH was sufficiently stable to survive the chromatographic isolation procedures that were required to obtain it in a pure state for analysis by NMR, it was found to be unstable under prolonged storage in deuterated chloroform, where it spontaneously converted to arteannuin X. This finding provided circumstantial evidence that arteannuin X might be biosynthesized from A-4,11-D via its tertiary hydroperoxide (A-4,11-DOOH) in vivo, in much the same way that DHAA has been shown to be transformed to artemisinin via the tertiary allylic hydroperoxide of DHAA, dihydroartemsinic acid tertiary hydroperoxide (DHAAOOH) (17).

In Planta Similarities Between the Synthesis of Arteannuin X and Artemisinin. Using UPLC-MS, we compared the conversion profile of A-4,11-D to arteannuin X in leaves with that of DHAA to artemisinin. Specifically, we also monitored DHAAOOH, the final intermediate in the in vivo production of artemisinin (Fig. 1 *A*, *iv* and *B*). We found that DHAAOOH levels peak in expanding WT leaves at a concentration of 0.5% leaf dry weight (Fig. 1 *A*, *iv* and Dataset S3). Artemisinin levels increase gradually from juvenile to mature leaves, reaching a maximum concentration of 1.2% dry leaf weight and remaining stable during the postharvest drying process. (Fig. 1 *A*, *iv* and Dataset S3). Previous work has shown that the DHAAOOH intermediate can also give rise to both dihydro-*epi*-deoxyarteannuin B (DHEDB) (31), and (by Hock-cleavage) deoxyartemisinin (17). Although DHEDB remains at a concentration threefold lower than artemisinin throughout leaf maturation and after harvest (Fig. 1 *A*, *vi* and Dataset S3), the levels of deoxyartemisinin increase during dry leaf storage, accumulating to 0.1% leaf dry weight (Fig. 1 *A*, *vii* and Dataset S3). These data suggest that, after harvest, any remaining DHAAOOH is preferentially converted to deoxyartemisinin rather than artemisinin.

We next carried out a more detailed analysis of the progression during leaf maturation of A-4,11-D to either arteannuin X or artemisinin in *cyp71av1-1* and WT, respectively, by performing ^{1}H NMR analysis on individual extracts from a 24-leaf maturation series (Fig. 2). Determination of the relative amounts of the three most abundant sesquiterpene metabolites associated with *cyp71av1-1* (A-4,11-D; A-4,11-DOOH; and arteannuin X) revealed a progressive decline in A-4,11-D, which was matched by an

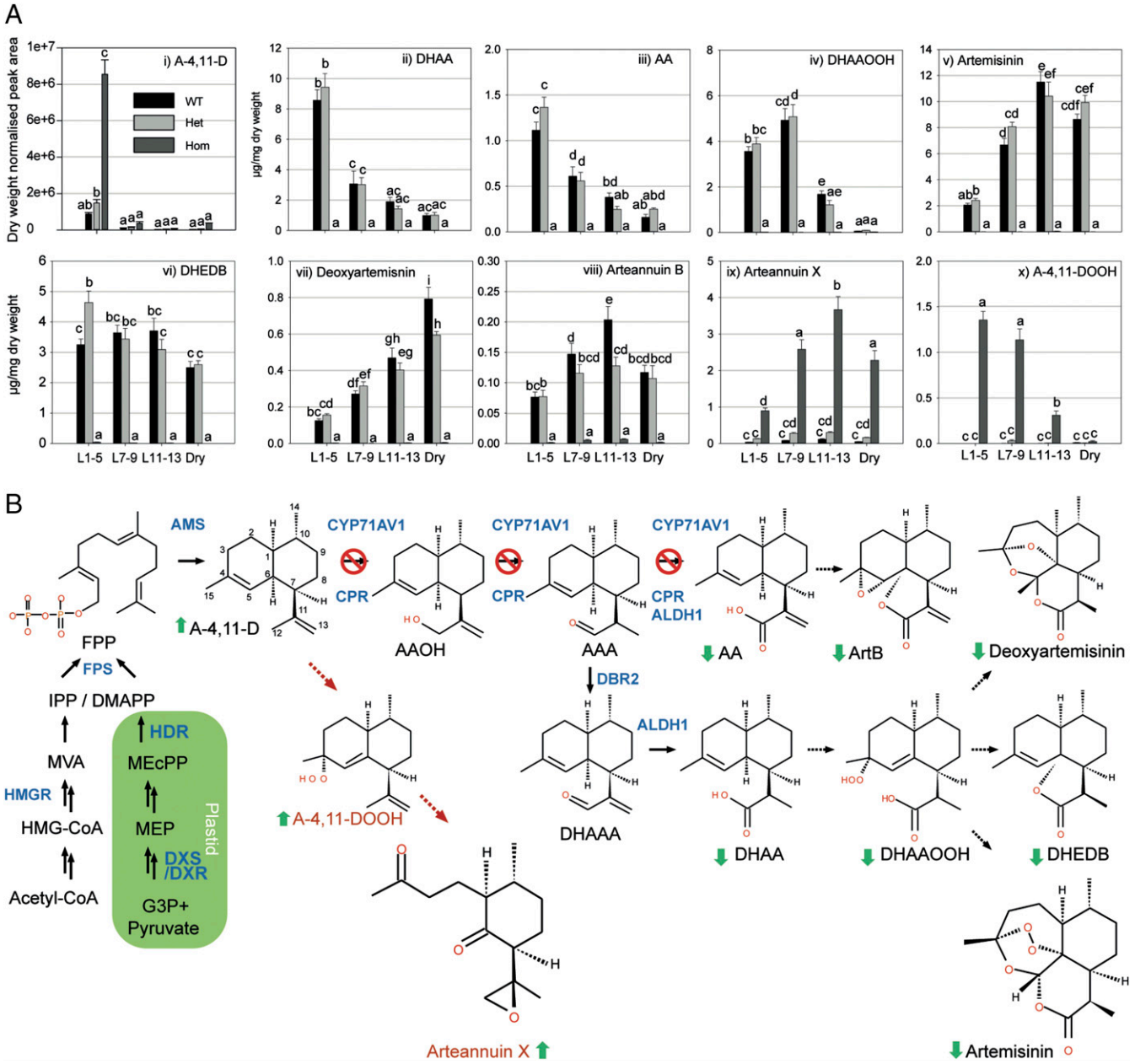

Fig. 1. Effects of *cyp71av1-1* mutation on selected sesquiterpene levels in fresh and dried leaves. (*A*) Level of selected sesquiterpenes were quantified by GC-MS (*i*) and UPLC-MS (*ii–x*) in fresh leaf (L) 1–5 (juvenile), 7–9 (expanding), and 11–13 (mature) as counted from the apical meristem, plus oven-dried whole plant-stripped leaves (dry) from 12-wk-old glasshouse-grown homozygous (hom), heterozygous (het) *cyp71av1-1*, and segregating WT as described in *SI Materials and Methods*. Error bars represent SEM ($n = 15$ for L1–5, L7–9, and L11–13; $n = 6$ for dry leaf). Letters represent Tukey's range test results after one-way ANOVA or restricted maximum likelihood (see *SI Materials and Methods* for details). Groups not sharing letters indicate statistically significant differences. (*B*) Summary of the effects of *cyp71av1-1* mutation on the level of selected sesquiterpenes. Red cross indicates steps of the pathway targeted by *cyp71av1-1* mutation. Full arrows, known enzymatic steps; dotted arrows, potential nonenzymatic conversions; brown dotted arrows, novel pathway operating in the *cyp71av1-1* mutant; full green arrows, metabolite changes (all types of leaves). AAA, artemisinic aldehyde; AAOH, artemisinic alcohol; ALDH1, aldehyde dehydrogenase; AMS, amorpha-4,11-diene synthase; ArtB, arteannuin B; CPR, cytochrome P450 reductase; DBR2, artemisinic aldehyde Δ 11(13) reductase; DeoxyArt, deoxyartemisinin; DHAAA, dihydroartemsinic aldehyde; DXR, 1-deoxy-D-xylulose-5-phosphate reductoisomerase; DXS, 1-deoxy-D-xylulose-5-phosphate synthase; FPP, farnesyl diphosphate; FPS, farnesyl diphosphate synthase; G-3-P, glyceraldehyde-3-phosphate; HDR, 4-hydroxy-3-methylbut-2-enyl diphosphate reductase; HMG-CoA, 3-hydroxy-3-methylglutaryl-CoA; HMGR, 3-hydroxy-3-methylglutaryl CoA reductase; MEcPP, 2-C-methyl-D-erythritol-2,4-cyclopyrophosphate; MEP, 2-C-methylerythritol 4-phosphate; MVA, mevalonate.

increase in arteannuin X. This analysis also demonstrated that the amount of A-4,11-DOOH reaches a maximum in leaves 7–8 (Fig. 2*A*). This pattern is entirely consistent with our hypothesis that A-4,11-D is converted to arteannuin X via the intermediate A-4,11-DOOH. ^{1}H NMR analysis of WT material clearly demonstrated that a decline in DHAA inversely correlates with an increase in artemisinin, which reaches a maximum at leaves 14–15, whereas the DHAAOOH intermediate peaks around leaves 7–8 (Fig. 2*B*), as for A-4,11-DOOH.

The results of the above experiments revealed clear parallels in the conversion of A-4,11-D to arteannuin X via the hydroperoxide intermediate (A-4,11-DOOH) and the final steps in the conversion of DHAA to artemisinin via DHAAOOH. There is strong in vivo and in vitro evidence for a nonenzymatic autoxidation

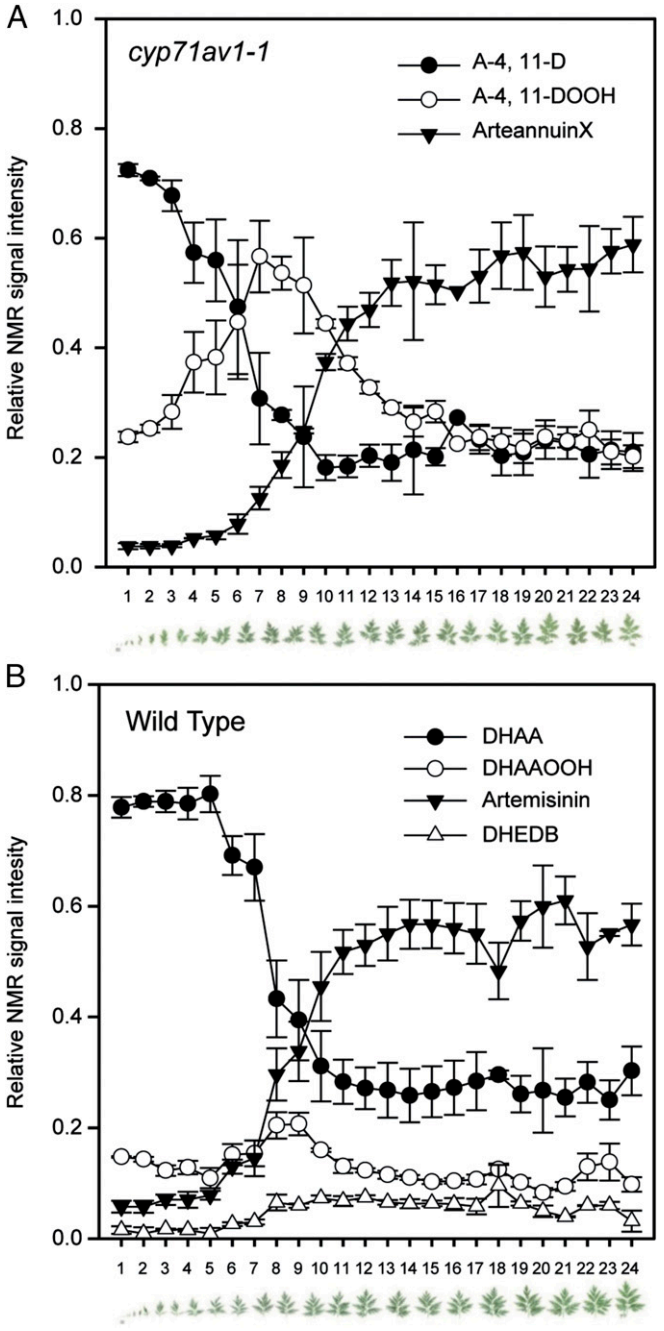

Fig. 2. Developmental patterns of artemisinin and arteannuin X biosynthesis. Leaves 1–24 (counting from apical meristem and shown below graphs) detached from the main stem of three *cyp71av1-1* (*A*) and three WT (*B*) plants. Chloroform extracts were subjected to NMR analysis (see *SI Materials and Methods* for details), and abundance for selected metabolites calculated from the integration of distinctive resonances is shown as proportion of the total for each leaf. Error bars, SEM ($n = 3$).

of DHAA to DHAAOOH and subsequent nonenzymatic rearrangement to artemisinin (17). Our data suggest that a similar autooxidation operates in *cyp71av1-1* to convert A-4,11-D to A-4,11-DOOH and on to arteannuin X. The spontaneous conversion of A-4,11-DOOH to arteannuin X in deuterated chloroform noted above is entirely consistent with this hypothesis. A speculative pathway to account for this conversion is detailed in Fig. S6.

In Vivo Evidence for Nonenzymatic DHAA Conversion in *cyp71av1-1* and WT Trichomes. Previous reports have suggested that peroxidase and/or dioxygenase enzymes may be involved in the conversion of DHAA to artemisinin (16, 32). To further investigate DHAA conversion, we fed [U-$^{13}C_{15}$]-DHAA to boiled, intact, and dark-incubated trichomes that had been isolated from *cyp71av1-1* (which lacks endogenous DHAA) and WT leaves (see *SI Materials and Methods* and Figs. S7–S9 for details). Chloroform extracts of [U-$^{13}C_{15}$]-DHAA–fed trichomes and no-trichome controls were subjected to UPLC-MS analysis, and the mass spectrum of each sesquiterpene ^{12}C monoisotope metabolite was used to predict the mass spectra expected from the corresponding [U-$^{13}C_{15}$]-isotopomer. Metabolite concentrations were first normalized to the trichome density for a given sample. Because DHAA can slowly degrade and convert spontaneously to "downstream" products over time, labeled metabolite concentrations in trichome samples were also corrected by subtracting concentrations measured in matched time-equivalent buffer controls. (Fig. 3).

It was found that [U-$^{13}C_{15}$]-artemisinin did not accumulate substantially over the 5-d feeding period in extracts of [U-$^{13}C_{15}$]-DHAA–fed trichomes in either *cyp71av1-1* or WT leaves (Fig. 3 *A* and *B*, white, red, and black triangles). Lack of artemisinin accumulation in trichomes fed with [U-$^{13}C_{15}$]-DHAA is perhaps not surprising, because previous results have indicated that DHAAOOH cannot efficiently undergo Hock cleavage into artemisinin in an aqueous environment (such as trichome extraction buffer) and that it may preferentially form DHEDB (17). We found an accumulation of [U-$^{13}C_{15}$]-DHEDB in extracts from both light-incubated boiled and intact trichomes from *cyp71av1-1* and WT leaves (Fig. 3 *A* and *B*, white and red squares). Dark-incubated samples did not show an accumulation of the [U-$^{13}C_{15}$]-labeled DHEDB (Fig. 3 *A* and *B*, black squares), leading us to conclude that DHEDB formation is light-dependent. Both *cyp71av1-1* and WT trichomes showed very similar patterns of [U-$^{13}C_{15}$]-DHEDB accumulation, which reached a plateau between 2 and 3 d after feeding commenced (Fig. 3 *A* and *B*, white and red squares). It is also evident that boiling accelerates the formation of DHEDB in both *cyp71av1-1* and WT trichomes (Fig. 3 *A* and *B*, red vs.. white squares), consistent with the process being nonenzymatic. We did not detect labeled DHAAOOH itself, which suggests that the experimental conditions favored rapid conversion of this intermediate through to DHEDB.

To investigate whether uptake of [U-$^{13}C_{15}$]-DHAA into isolated trichomes is a limiting factor in the feeding experiment, we fed the labeled substrate to crude protein extracts from isolated trichomes. The products and temporal pattern of their accumulation was very similar to that obtained for the intact trichome feeding (Fig. 3 *C* and *D*). Notably, there was no accumulation of [U-$^{13}C_{15}$]-artemisinin over the 5-d feeding period (Fig. 3 *C* and *D*, red, black, and white triangles), whereas [U-$^{13}C_{15}$]-DHEDB accumulated in both light-incubated boiled and nonboiled protein extracts from *cyp71av1-1* and WT trichomes (Fig. 3 *C* and *D*, red and white squares). It is also evident that boiling accelerates the formation of DHEDB in both *cyp71av1-1* and WT trichome protein extracts (Fig. 3 *C* and *D*, red vs. white squares), consistent with the process being nonenzymatic.

The intact trichome-feeding and trichome protein extract-feeding experiments demonstrate that in *cyp71av1-1*, a block in artemisinin and DHEDB biosynthesis can be rescued by direct feeding of DHAA, which is expected, given the role of CYP71AV1 in the artemisinin biosynthetic pathway (Fig. 1*B*). The lack of further accumulation of artemisinin over a 5-d period in trichomes maintained in an aqueous medium contrasts with the gradual accumulation of artemisinin in trichomes during leaf maturation (Figs. 1 and 2). These observations lead us to suggest that the nonaqueous environment present in the intact subapical cavity of glandular secretory trichomes is essential for the efficient conversion of DHAA to artemisinin via DHAAOOH. In the absence of

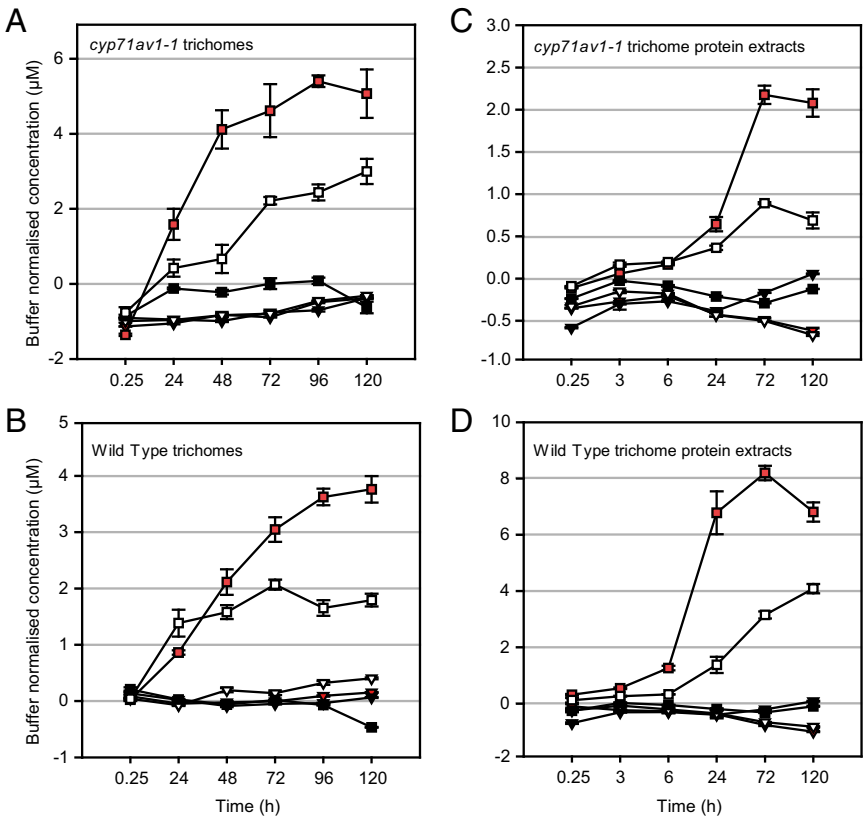

Fig. 3. Feeding intact and protein-extracted glandular secretory trichomes (GSTs) with ^{13}C-isotope–labeled DHAA. Intact GSTs isolated from young leaves of *cyp71av1-1* (*A*) or segregating WT (*B*) and trichome protein extracts from *cyp71av1-1* (*C*) or segregating WT (*D*) were fed with [U-$^{13}C_{15}$]-DHAA as described in *SI Materials and Method*. The concentration of selected [U-$^{13}C_{15}$]-labeled metabolites was first corrected for the different densities of the GST extracts and then calculated with subtraction of relevant feeding buffer controls, containing no trichomes or protein extracts. Metabolites are represented by shapes: artemisinin, triangles; DHEDB, squares. Treatments are represented by colors: white, intact, light-incubated GSTs; black, intact, dark-incubated GSTs; red, boiled, light-incubated GSTs. Level of metabolites was monitored by UPLC-MS. See *SI Materials and Methods* for details. Error bars, SEM (n = 3). Labeled substrate ([U-$^{13}C_{15}$]-DHAA) levels started at a concentration of 30–40 μM (off the scale of the graphs) and decreased as expected over the course of the experiments.

such an environment, DHAA is instead converted to DHEDB in a light-dependent nonenzymatic process.

The hydrophobic nature of A-4,11-D prevented us from preparing aqueous solutions of [U-$^{13}C_{15}$]-A-4,11-D for trichome-feeding experiments and performing a similar analysis of arteannuin X in the *cyp71av1-1* mutant.

Given that the final steps in artemisinin biosynthesis appear to be nonenzymatic, the question arises as to how its production during leaf maturation is controlled. It is reasonable to assume that active transport system(s) will be responsible for pumping artemisinin precursors into the subapical cavity of glandular secretory trichomes. Transport of DHAA into the subapical cavity could be a limiting factor, with spatial and temporal expression patterns of relevant transporters controlling the increase in artemisinin during leaf maturation (Fig. 2*B*).

Conclusion

We have described an *A. annua CYP71AV1* knockout mutant that provides in planta confirmation for the function of this enzyme. The *cyp71av1-1* mutant accumulates high levels of A-4,11-D, which is converted to arteannuin X, a *nor- seco*-amorphane sesquiterpene epoxide. This work clearly demonstrates the plasticity of metabolism in the glandular secretory trichomes of *A. annua*; when one pathway is blocked, novel sesquiterpene alternatives are produced, highlighting the potential of trichomes as factories for production of new compounds with potential medicinal and industrial applications.

We found that the in vivo oxidation of A-4,11-D to arteannuin X parallels that of DHAA to artemisinin during the progression of leaf maturation. We were able to chemically complement *cyp71av1-1* by externally feeding DHAA to intact trichome preparations and trichome protein extracts. This finding demonstrated that the conversion of DHAA to DHEDB, via a tertiary allylic hydroperoxide, is a nonenzymatic, light-requiring process. The lack of accumulation of artemisinin in these experiments supports the idea that a nonaqueous environment, as provided by the subapical cavity of glandular secretory trichomes, is essential for the nonenzymatic production of the endoperoxide containing artemisinin from DHAA. Together, these findings highlight the importance of nonenzymatic conversions in terpenoid metabolism of *A. annua* glandular secretory trichomes. These findings, together with the observation that artemisinin is known to be cytotoxic to various cell types (4, 33, 34), suggest a functional requirement for the specialized subapical cavity as a location for both chemical conversion and storage. It also highlights the challenges of producing certain types of plant natural products in microbial systems that lack this level of structural complexity and the need for more research into the compartmentation of metabolic processes in plant production systems.

Materials and Methods

Full details of plant material used, plant growth conditions, screening of EMS-mutagenized population, genotyping, metabolomic analyses, 2D NMR

structural characterization, trichome extractions, and trichome feeding with ^{13}C-labeled substrates are presented in *SI Materials and Methods*.

ACKNOWLEDGMENTS. We thank C. Paddon and K. Monroe (Zagaya) for providing [U-$^{13}C_{15}$]-(uniformly) labeled A-4,11-D and DHAA; T. Winzer for preliminary experimental involvement; L. Doucet, D. Vyas, C. Whitehead, and B. Kowalik, for laboratory assistance; C. Abbot and A. Fenwick for horticulture assistance; P. Roberts for graphic design; C. Calvert for project management; and X. Simonnet and Médiplant for access to the Artemis variety. G.D.B. thanks the Chemical Analysis Facility at the University of Reading for provision of the 700-MHz NMR spectrometer used in these studies. This work was supported by The Bill and Melinda Gates Foundation and by Biotechnology and Biological Sciences Research Council Grant BB/G008744/1 (to G.D.B.), "The Biosynthesis of Artemisinin."

1. Duke SO, Paul RN (1993) Development and fine structure of the glandular trichomes of *Artemisia annua* L. *Int J Plant Sci* 154(1):107–118.
2. Duke MV, Paul RN, Elsohly HN, Sturtz G, Duke SO (1994) Localization of artemisinin and artemisitene in foliar tissues of glanded and glandless biotypes of *Artemisia-Annua* L. *Int J Plant Sci* 155(3):365–372.
3. Olsson ME, et al. (2009) Localization of enzymes of artemisinin biosynthesis to the apical cells of glandular secretory trichomes of *Artemisia annua* L. *Phytochemistry* 70(9):1123–1128.
4. Yan ZQ, et al. (2015) Mechanism of artemisinin phytotoxicity action: Induction of reactive oxygen species and cell death in lettuce seedlings. *Plant Phys Biochem* 88: 53–59.
5. Lange BM, Ahkami A (2013) Metabolic engineering of plant monoterpenes, sesquiterpenes and diterpenes—current status and future opportunities. *Plant Biotechnol J* 11(2):169–196.
6. Lange BM, Turner GW (2013) Terpenoid biosynthesis in trichomes—current status and future opportunities. *Plant Biotechnol J* 11(1):2–22.
7. Lapkin AA, Plucinski PK, Cutler M (2006) Comparative assessment of technologies for extraction of artemisinin. *J Nat Prod* 69(11):1653–1664.
8. Paddon CJ, Keasling JD (2014) Semi-synthetic artemisinin: A model for the use of synthetic biology in pharmaceutical development. *Nat Rev Microbiol* 12(5):355–367.
9. Paddon CJ, et al. (2013) High-level semi-synthetic production of the potent antimalarial artemisinin. *Nature* 496(7446):528–532.
10. Turconi J, et al. (2014) Semisynthetic artemisinin, the chemical path to industrial production. *Org Process Res Dev* 18(3):417–422.
11. Peplow M (2016) Synthetic biology's first malaria drug meets market resistance. *Nature* 530(7591):389–390.
12. Mercke P, Bengtsson M, Bouwmeester HJ, Posthumus MA, Brodelius PE (2000) Molecular cloning, expression, and characterization of amorpha-4,11-diene synthase, a key enzyme of artemisinin biosynthesis in *Artemisia annua* L. *Arch Biochem Biophys* 381(2):173–180.
13. Teoh KH, Polichuk DR, Reed DW, Nowak G, Covello PS (2006) *Artemisia annua* L. (Asteraceae) trichome-specific cDNAs reveal CYP71AV1, a cytochrome P450 with a key role in the biosynthesis of the antimalarial sesquiterpene lactone artemisinin. *FEBS Lett* 580(5):1411–1416.
14. Zhang Y, et al. (2008) The molecular cloning of artemisinic aldehyde Delta11(13) reductase and its role in glandular trichome-dependent biosynthesis of artemisinin in *Artemisia annua*. *J Biol Chem* 283(31):21501–21508.
15. Teoh KH, Polichuk DR, Reed DW, Covello PS (2009) Molecular cloning of an aldehyde dehydrogenase implicated in artemisinin biosynthesis in *Artemisia annua*. *Botany* 87(6):635–642.
16. Soetaert SS, et al. (2013) Differential transcriptome analysis of glandular and filamentous trichomes in *Artemisia annua*. *BMC Plant Biol* 13:220.
17. Brown GD, Sy L-K (2004) In vivo transformations of dihydroartemisinic acid in *Artemisia annua* plants. *Tetrahedron* 60(5):1139–1159.
18. Sy LK, Brown GD (2002) The role of the 12-carboxyllic acid group in the spontaneous autoxidation of dihydroartemisinic acid. *Tetrahedron* 58(5):909–923.
19. Graham IA, et al. (2010) The genetic map of *Artemisia annua* L. identifies loci affecting yield of the antimalarial drug artemisinin. *Science* 327(5963):328–331.
20. Larson TR, et al. (2013) A survey of artemisinic and dihydroartemisinic acid contents in glasshouse and global field-grown populations of the artemisinin-producing plant *Artemisia annua* L. *Ind Crops Prod* 45:1–6.
21. Brown GD (2010) The biosynthesis of artemisinin (Qinghaosu) and the phytochemistry of *Artemisia annua* L. (Qinghao). *Molecules* 15(11):7603–7698.
22. Ivanescu B, Miron A, Corciova A (2015) Sesquiterpene lactones from artemisia genus: Biological activities and methods of analysis. *J Anal Methods Chem* 2015:247685.
23. Wang W, Wang Y, Zhang Q, Qi Y, Guo D (2009) Global characterization of *Artemisia annua* glandular trichome transcriptome using 454 pyrosequencing. *BMC Genomics* 10:465.
24. Weng JK, Philippe RN, Noel JP (2012) The rise of chemodiversity in plants. *Science* 336(6089):1667–1670.
25. Ma DM, et al. (2015) A genome-wide scenario of terpene pathways in self-pollinated *Artemisia annua*. *Mol Plant* 8(11):1580–1598.
26. Ro DK, et al. (2006) Production of the antimalarial drug precursor artemisinic acid in engineered yeast. *Nature* 440(7086):940–943.
27. Komori A, et al. (2013) Comparative functional analysis of CYP71AV1 natural variants reveals an important residue for the successive oxidation of amorpha-4,11-diene. *FEBS Lett* 587(3):278–284.
28. McCallum CM, Comai L, Greene EA, Henikoff S (2000) Targeting induced local lesions IN genomes (TILLING) for plant functional genomics. *Plant Physiol* 123(2):439–442.
29. Lommen WJ, Schenk E, Bouwmeester HJ, Verstappen FW (2006) Trichome dynamics and artemisinin accumulation during development and senescence of *Artemisia annua* leaves. *Planta Med* 72(4):336–345.
30. Olofsson L, Engström A, Lundgren A, Brodelius PE (2011) Relative expression of genes of terpene metabolism in different tissues of *Artemisia annua* L. *BMC Plant Biol* 11:45.
31. Sy LK, Zhu NY, Brown GD (2001) Syntheses of dihydroartemisinic acid and dihydro-epi-deoxyarteannuin B incorporating a stable isotope labe at the 15-position for studies into the biosynthesis of artemisinin. *Tetrahedron* 57(40):8495–8510.
32. Bryant L, Flatley B, Patole C, Brown GD, Cramer R (2015) Proteomic analysis of *Artemisia annua*—towards elucidating the biosynthetic pathways of the antimalarial pro-drug artemisinin. *BMC Plant Biol* 15:175.
33. Knudsmark Jessing K, Duke SO, Cedergreeen N (2014) Potential ecological roles of artemisinin produced by *Artemisia annua* L. *J Chem Ecol* 40(2):100–117.
34. Li W, et al. (2005) Yeast model uncovers dual roles of mitochondria in action of artemisinin. *PLoS Genet* 1(3):e36.
35. Delabays N, Simonnet X, Gaudin M (2001) The genetics of artemisinin content in *Artemisia annua* L. and the breeding of high yielding cultivars. *Curr Med Chem* 8(15): 1795–1801.
36. Townsend T, et al. (2013) The use of combining ability analysis to identify elite parents for *Artemisia annua* F1 hybrid production. *PLoS One* 8(4):e61989.
37. Till BJ, Zerr T, Comai L, Henikoff S (2006) A protocol for TILLING and Ecotilling in plants and animals. *Nat Protoc* 1(5):2465–2477.
38. Ruijter JM, et al. (2009) Amplification efficiency: Linking baseline and bias in the analysis of quantitative PCR data. *Nucleic Acids Res* 37(6):e45.
39. Smith CA, Want EJ, O'Maille G, Abagyan R, Siuzdak G (2006) XCMS: Processing mass spectrometry data for metabolite profiling using nonlinear peak alignment, matching, and identification. *Anal Chem* 78(3):779–787.
40. Tautenhahn R, Böttcher C, Neumann S (2008) Highly sensitive feature detection for high resolution LC/MS. *BMC Bioinformatics* 9:504.
41. Kuhl C, Tautenhahn R, Böttcher C, Larson TR, Neumann S (2012) CAMERA: An integrated strategy for compound spectra extraction and annotation of liquid chromatography/mass spectrometry data sets. *Anal Chem* 84(1):283–289.
42. Guha R (2007) Chemical informatics functionality in R. *J Stat Softw* 18(5).
43. Stacklies W, Redestig H, Scholz M, Walther D, Selbig J (2007) pcaMethods—a bioconductor package providing PCA methods for incomplete data. *Bioinformatics* 23(9): 1164–1167.
44. McCaskill D, Croteau R (1995) Monoterpene and sesquiterpene biosynthesis in glandular trichomes of peppermint (*Mentha* X *Piperita*) rely exclusively on plastid-derived isopentenyl diphosphate. *Planta* 197(1):49–56.
45. Westfall PJ, et al. (2012) Production of amorphadiene in yeast, and its conversion to dihydroartemisinic acid, precursor to the antimalarial agent artemisinin. *Proc Natl Acad Sci USA* 109(3):E111–E118.
46. Yang J, et al. (2015) The I-TASSER Suite: Protein structure and function prediction. *Nat Methods* 12(1):7–8.